Physica Medica 62 (2019) 63–72

Contents lists available at ScienceDirect

Physica Medica

journal homepage: www.elsevier.com/locate/ejmp

Original paper

Rotational radiotherapy of breast cancer with polyenergetic kilovoltage X-ray beams: An experimental and Monte Carlo phantom study

F. Buonanno[a,b], A. Sarno[a,b], P.A. De Lucia[a,1], F. Di Lillo[a,b], M. Masi[a,b,2], F. Di Franco[a,b], G. Mettivier[a,b,*], P. Russo[a,b]

[a] Università di Napoli Federico II, Dipartimento di Fisica "Ettore Pancini", I-80126 Napoli, Italy
[b] INFN Sezione di Napoli, I-80126 Napoli, Italy

ARTICLE INFO

Keywords:
Breast cancer
Rotational kilovoltage radiotherapy
Computed tomography
Monte Carlo simulations

ABSTRACT

Purpose: We investigated the feasibility of kilovoltage rotational radiotherapy for breast cancer (kV-EBRT) via Monte Carlo simulations and measurements on phantoms.
Methods: We derived the dose distributions for X-ray beams at 150 kV, 300 kVp and 320 kV irradiating breast cylindrical phantoms of 14 cm diameter, mimicking the pendant breast. Simulations were based on the Geant4 toolkit. The point-like X-ray source was rotated either over a full circle or on a limited arc around the phantom. We studied the influence on the surface dose of the distance between the tumor lesion to the skin, of the irradiation protocol (full scan or partial scan) and of the X-ray tube current modulation.
Results: Rotational kV-EBRT permitted a periphery-to-center dose ratio from 13% to 9% in homogeneous breast phantoms. Dose distributions in phantoms with off-center simulated lesions, showed a skin-to-tumor dose ratio of 16% and 34% for lesions at 3.25 and 5.25 cm from cylinder axis, respectively. Simulation of the X-ray tube current modulation during the rotation, permits to reach a dose ratio of 20% for the lesion located at 5.25 cm from phantom axis.
Conclusions: We showed the possibility of using low-energy X-ray spectra for kV-EBRT with collimated beams, for obtaining a periphery-to-center dose ratio in the same order of conventional accelerator based megavoltage radiotherapy, when the irradiated area is localized in the center of the breast. For tumors localized near the breast border, we showed that the tube current modulation can be a good solution in order to reduce the skin-to-tumor dose ratio.

1. Introduction

In 2012, in a pioneering paper [1], the UC Davis team showed the proof-of-principle for a new technique for external beam radiotherapy (EBRT) of breast cancer. This technique (kV-EBRT) utilizes kilovoltage (kV) X-rays photon beams produced by an orthovoltage X-ray tube, rather than irradiation with megavoltage (MV) tangential beams with the woman in supine position, as in conventional accelerator based EBRT. In principle, kilovoltage photon beams (e.g. 320 kV with 4 mm Cu filtration) are inadequate for producing the desirable dose skin sparing effect achievable with MV X-ray beams, due to the absence of the dose build-up region between $z = 0$ and z_{max} (with maximum dose D_{max} located at $z_{max} \cong 1.5$ cm and surface dose $D_s \cong 15\%$ of the maximum dose, for a $10 \times 10\,cm^2$ 6 MV X-ray beam) [2]. In order to overcome this problem, on the basis of detailed Monte Carlo (MC) simulations, the UC Davis team proposed to deliver the target dose during a full rotation of a *suitably-collimated* kV source around the tumor. The beam from the X-ray tube is collimated in the horizontal and vertical planes to cover the size of the target and rotates in a circular orbit around the pendant breast of the woman in prone position. This irradiation modality permits to lower the skin dose, achieving a percentage skin-to-tumor dose ratio of less than 10%, for an average breast (14 cm diameter at chest wall) and a centrally located lesion. Hence, rotational summation of the dose would permit the delivery of high doses to a tumor target in the breast while reducing the dose to the skin. The implementation of this new rotational kV-EBRT technique on the same platform of a dedicated breast computed tomography (BCT) scanner for breast cancer diagnosis [3,4] would provide a complete

* Corresponding author.
E-mail address: mettivier@na.infn.it (G. Mettivier).
[1] Present address: Malzoni Radiosurgery Center, via Marrota 1, I-84043, Agropoli (Salerno), Italy.
[2] Present address: Università di Roma "Tor Vergata", Sez. di Fisica Medica, I-00133 Roma, Italy.

https://doi.org/10.1016/j.ejmp.2019.05.002
Received 5 February 2019; Received in revised form 1 May 2019; Accepted 2 May 2019
Available online 09 May 2019

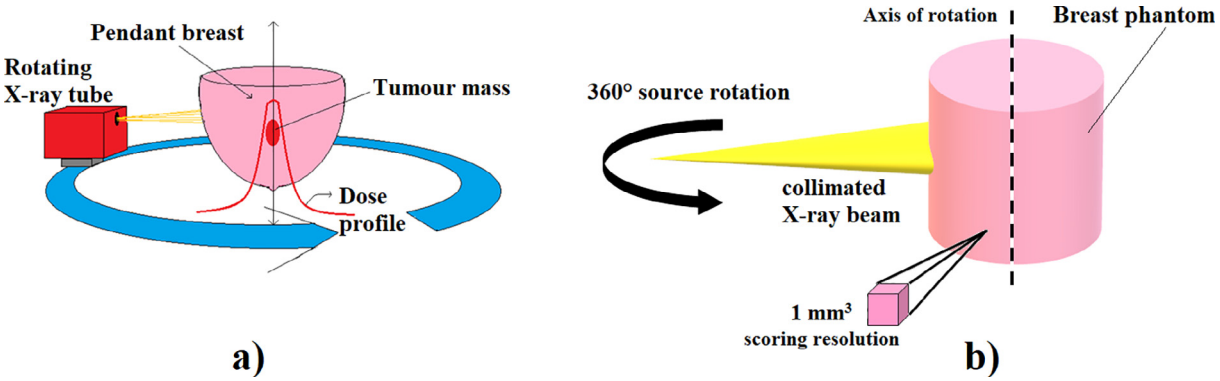

Fig. 1. a) Scheme for rotational kilovoltage external beam radiotherapy with an X-ray tube rotating around the pendant breast of the woman in prone position, with the axis of rotation passing through the tumor lesion. The principle of rotational summation of the dose produces a reversal of the single-view decreasing dose profile vs. depth in the organ, whereby a dose peak is generated at the axis of rotation and a reduced dose occurs at the surface of the breast. b) In the simulations, the breast was modelled as a polyethylene cylinder with voxels of 0.1 cm^3 size, and the collimated X-ray beam rotating around the phantom.

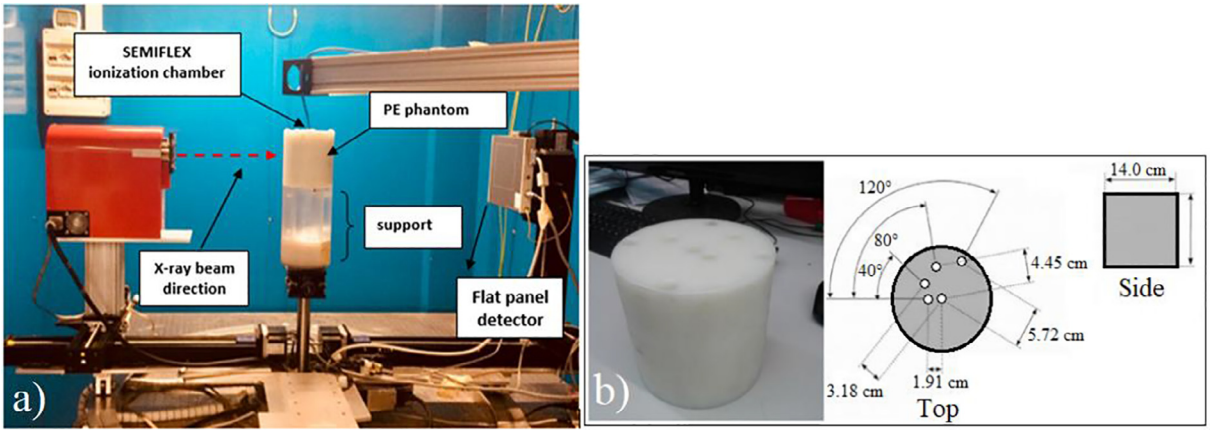

Fig. 2. a) Experimental setup for 150 kV irradiation, adopting the BCT platform assembled at University & INFN Napoli. b) Polyethylene cylindrical phantom containing vertical holes for hosting an ionization chamber at various radial distances.

image guided EBRT setup [1]. This setup may represent a low-cost alternative to conventional breast radiotherapy (RT) thanks to a significant reduction of the cost of the radiation source (X-ray tube unit vs. linac) and to the avoidance of the accelerator bunker.

In conventional 3D conformal RT the whole breast volume is irradiated (whole breast irradiation, WBI), but techniques are under investigation where only a partial breast irradiation (PBI) is carried out, localized on the target volume [5]. WBI can be performed with kV-EBRT technique, by multiple rotations with different collimation width at each rotation [1] but this technique is particularly suited for PBI. Recently, the kV-EBRT technique for breast cancer PBI treatment – with the patient in the supine or prone position and with the kilovoltage source rotating on an arc − has been investigated using MC simulations by Bazalova-Carter and her team [6–8]. Their approach adopts a design 200-kV kilovoltage arc therapy (KVAT) large-area X-ray source and a collimator which produces a set of beamlets converging at the radiation isocenter. Such a source is still unavailable, but the envisaged application to breast RT is promising, confirming the advantages of the rotational technique in lowering the skin dose while suitably irradiating deep targets [7].

The UC Davis team validated this technique via measurements performed on their cone beam BCT scanner operated at 120 kV, 0.2 mm Cu filtration. A complete experimental validation of the rotational kV-EBRT technique at higher kV settings is not available, though.

In our previous papers [9,10], using mononergetic beams from a synchrotron radiation source, we investigated the technique proposed by the UC Davis group, both via Monte Carlo simulations and validation measurements. We showed the possibility of achieving a considerable skin sparing effect even with photon energies lower than those proposed in Ref. [1]: for energies down to 60 keV a skin-to-tumor dose ratio of 14% was demonstrated. For the same breast model and irradiation geometry, such a dose ratio reduced to about 10% at 175 keV, close to the effective energy of the beam adopted in Ref. [1] (178 keV).

In this work, we perform a full validation of the kV-EBRT technique. In particular, we explored via MC simulations, as well as via experimental measurements on a prototype scanner and on phantoms, the possibility of a further reduction of the adopted photon energy for polyenergetic spectra at 300 kVp and 150 kV produced by conventional X-ray tubes. In addition, we investigated the 3D distribution of the scatter dose in out-of-target planes as well as the dose homogeneity in the target volume. We also explored the possibility of PBI with gantry rotation for a scan angle less than 360 deg and the effects of tube current modulation on dose distribution and dose sparing. The results of this study confirm and extend the previous findings reported in [1,11], with the purpose of showing the possibility of using a wider range of tube voltages (from 320 kV down to 150 kV) than in the former UC Davis approach.

2. Materials and methods

2.1. Monte Carlo code

A rotational kV-EBRT treatment was simulated via a MC code with either monoenergetic or polyenergetic X-ray beams (Fig. 1a). The MC code was developed from a previous code written for simulating dose distributions in breast cancer treatment using synchrotron radiation

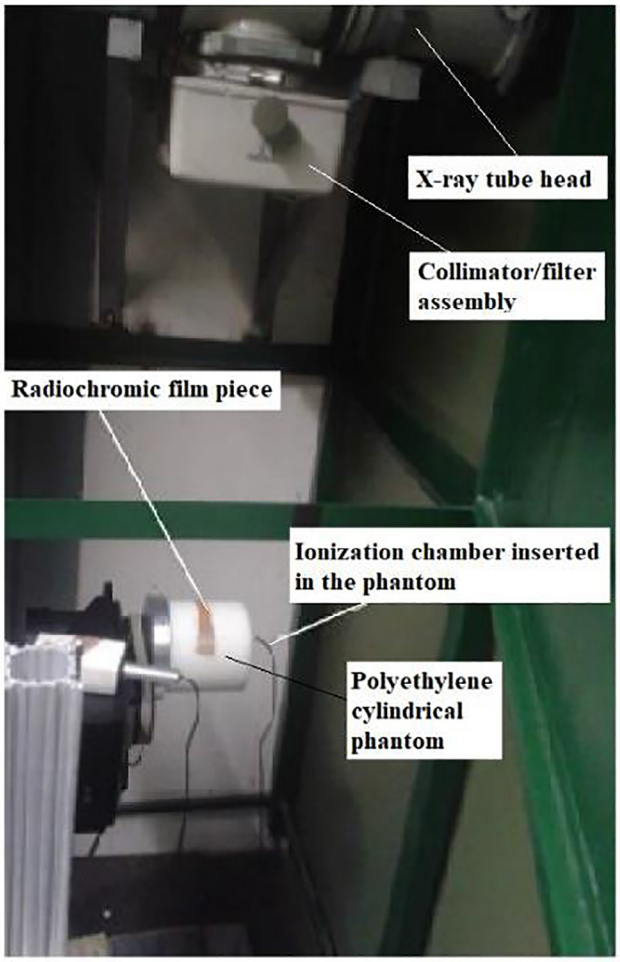

Fig. 3. Experimental setup for 300 kVp irradiation, using an orthovoltage X-ray tube. Here, the beam central axis is vertical, and the cylindrical PE phantom rotates around a horizontal axis. The incident beam area was measured using a radiochromic film piece.

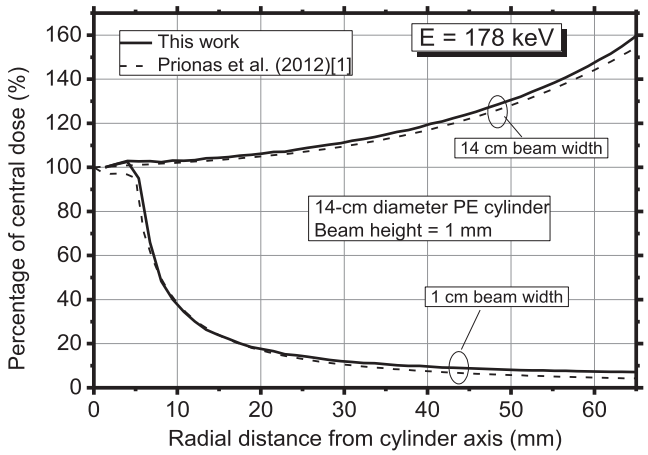

Fig. 5. Comparison between monoenergetic 178 keV MC simulations achieved in a 14-cm diameter PE cylinder in this work (solid lines) and that provided by Prionas et al. [1] (dashed lines) for 1 or 14 cm of horizontal beam width and 1 mm of vertical beam height. The graph shows percentage of central dose versus radial distance from isocenter.

[9,10] and dose estimates in X-ray breast imaging [12–14]. It was based on the GEANT4 toolkit (version 10.00) with the low energy physics list Option4. We simulated photoelectric, coherent and incoherent scatter photon interactions, with electron kinetic energy tracked down to 990 eV. The breast was modelled as a cylinder made either of polyethylene (PE) (which mimics the absorption in the breast adipose tissue at kilovoltage energies) or of a homogeneous mixture of glandular and adipose breast tissue with a glandular fraction by mass of 0%, 50% or 100%. The isotropic X-ray beam originated from a point source, collimated in order to irradiate a defined area at the isocenter (Fig. 1b). The tumor lesion was modelled as a cylinder with a diameter of 1.5 cm and made of breast tissue of given glandular fraction. The lesion was located in the central plane with its central axis at the scanner isocenter. The absorbed dose and the deposit location were scored in order to produce dose maps. The produced dose maps presented voxels of size $0.1 \times 0.1 \times 0.1\ cm^3$; dose values presented a statistical uncertainty lower than 1% in the directly irradiated volume.

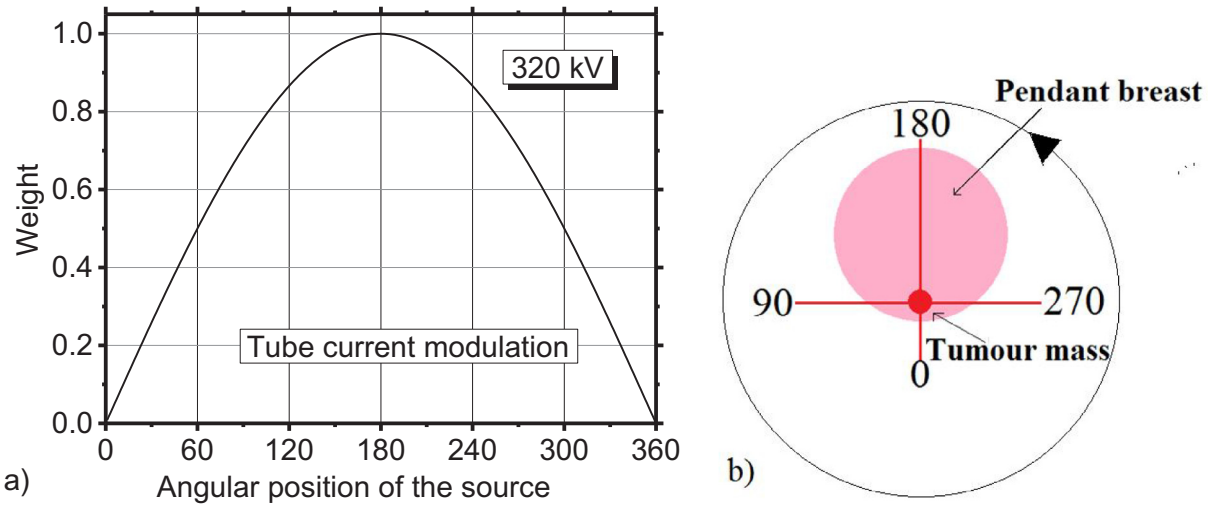

Fig. 4. a) Angular profile of the relative weight for tube current modulation (at 320 kV), following a sine function. b) Scheme (coronal view) of the irradiated breast (14 cm diameter) with a small tumor lesion placed at 5.25 cm from the central axis of the breast phantom. The X-ray tube position starts at angle 0 and goes on a circular orbit in a full rotation, while the tube current increases up to 180 deg and then decreases up to 360 deg following the profile in (a). The axis of rotation of the source is placed at the center of the lesion.

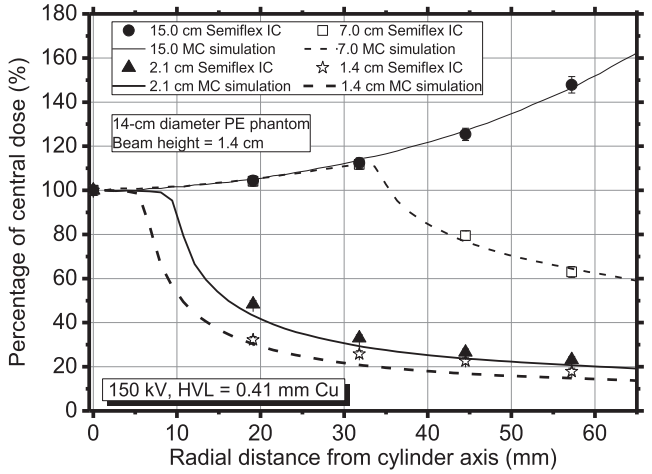

Fig. 6. Comparison between the measured (data point) and MC simulated (solid and dashed lines) radial profiles. Percentage of central dose was plotted as a function of the radial distance from the isocenter in a 14-cm diameter PE cylindrical phantom, for beam width of 1.4, 2.1, 7, 15 cm. Error bars on the graph indicate uncertainty of measurements. Tube voltage: 150 kV, HVL = 0.41 mm Cu.

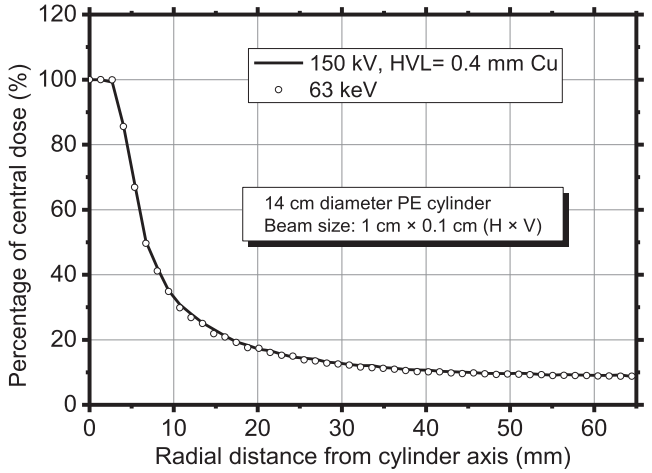

Fig. 7. Simulated radial dose profiles. The profile (continuous line) corresponds to the irradiation of a 14 cm PE cylinder with a 150 kV (HVL = 0.41 mm Cu) X-ray spectrum. Data points (circles) are for a 63 keV monoenergetic X-ray spectrum.

2.2. Validation of the MC code

The previous versions of the MC code adopted in this work were validated vs. data provided in the report of AAPM Task Group 195 [15,16] and vs. measured data with low energy [12] as well as high energy cases [9,10]. However, since it presents slight modifications compared to previous versions, we provided a further validation of the code by replicating simulations in Ref. [1]. We simulated a 178-keV monoenergetic X-ray source irradiating a PE cylinder (14.0 cm diameter, 9 cm height). The cylinder axis was coincident with the rotation axis of the system. The beam size was 14.0 × 0.1 cm^2 or 1.0 × 0.1 cm^2 (H × V) and the dose was scored in a 3D matrix with 0.1 cm^3 isotropic voxels [1].

2.3. Dose distribution at 150 kV

The configuration adopted in Ref. [1] was replicated in order to simulate dose distributions within the simulated breast model both in coronal and sagittal planes.

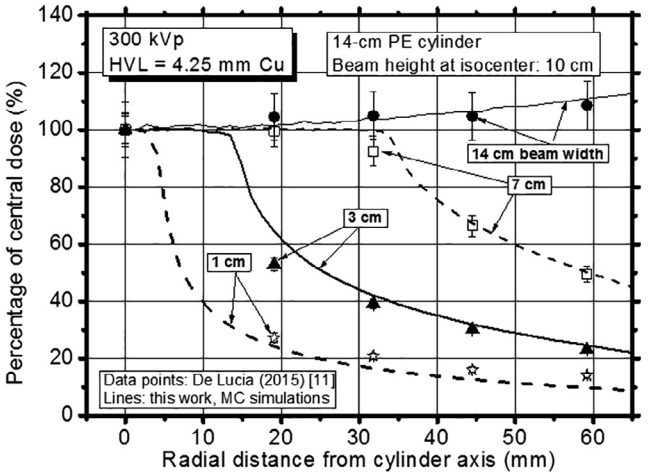

Fig. 8. Comparison between measured (data point) vs simulated dose distributions (solid and dashed lines). Radial dose profiles for different beam widths were obtained. For the MC simulated dose distributions, the radial profiles were calculated along 10 cm at the cylinder axis. The measurements were performed in a previous work [11] with a 10 cm ionization chamber. Tube voltage: 300 kVp, HVL = 4.25 mm Cu.

Measurements at 150 kV were performed with a bench-top BCT scanner prototype, available at our laboratory, which embodies an X-ray tube (Hamamatsu L8121-03) which operates at a constant voltage up to 150 kV [4].

Measurements of radial dose profiles were performed with a 0.0125 cm^3 Semiflex type ionization chamber (IC) (mod. 31010, PTW Freiburg GmbH, Germany) in a homogenous PE cylinder (0.9325 g/cm^3) (14 cm diameter, 15 cm height). Cylindrical holes (1.3 cm diameter) were drilled in the phantom to host the IC (Fig. 2) at different distances from the cylinder axis (0, 1.91, 3.18, 4.45 cm, respectively). The IC was factory calibrated with a Co^{60} beam with an accuracy ≤ ± 5% at 150 kV. The X-ray spectrum at 150 kV was filtered with 0.2 mm of copper (HVL = 0.41 mm Cu, or 7.45 mm Al) and two pairs of tungsten blades were used to collimate the X-ray beam in the horizontal and vertical direction, respectively. The cylinder axis was coincident with the rotation axis of the system. The IC was irradiated at each position during a complete rotation over 360 degrees. During the irradiation, PE rods filled the unutilized holes. The experiment was replicated for different beam collimations. The beam height in the axial direction was fixed at 1.4 cm at isocenter, in order to expose the entire sensitive volume of the ion chamber while the X-ray beam was collimated to 1.4, 2.1, 7.0, or 15.0 cm in the horizontal plane (measured at isocenter). The corresponding MC code was produced with a scoring spatial resolution of 0.1 × 0.1 × 0.1 cm^3. For every MC simulation we launched 10^8 photons. We investigated also the possibility of using a monoenergetic beam at the effective energy of the 150 kV spectrum. For this purpose, the simulated radial dose profile at 150 kV in PE was matched with that simulated at the effective energy of the spectrum.

2.4. Dose distribution at 300 kVp

In addition, the 3D dose distribution within the PE cylindrical phantom (diameter of 14 cm and height of 15 cm) was measured for irradiation by means of a Siemens Stabilipan 2 orthovoltage X-ray tube (filtration 1 mm Al + 3.37 mm Cu + 1.2 mm Sn) adopted in a preliminary investigation [11]. It operated at 300 kVp (HVL = 4.25 mm Cu, or 20 mm Al) (with a ripple of 5%). The beam was collimated in order to have, at the scanner isocenter, an irradiation field of 10 cm in the vertical direction, in order to match the height of the adopted ion chamber (3 cm^3 ionization chamber - mod. Radcal 20X6-3CT, dosimeter Radcal 2026C, Monrovia, CA, USA). The beam was collimated in the

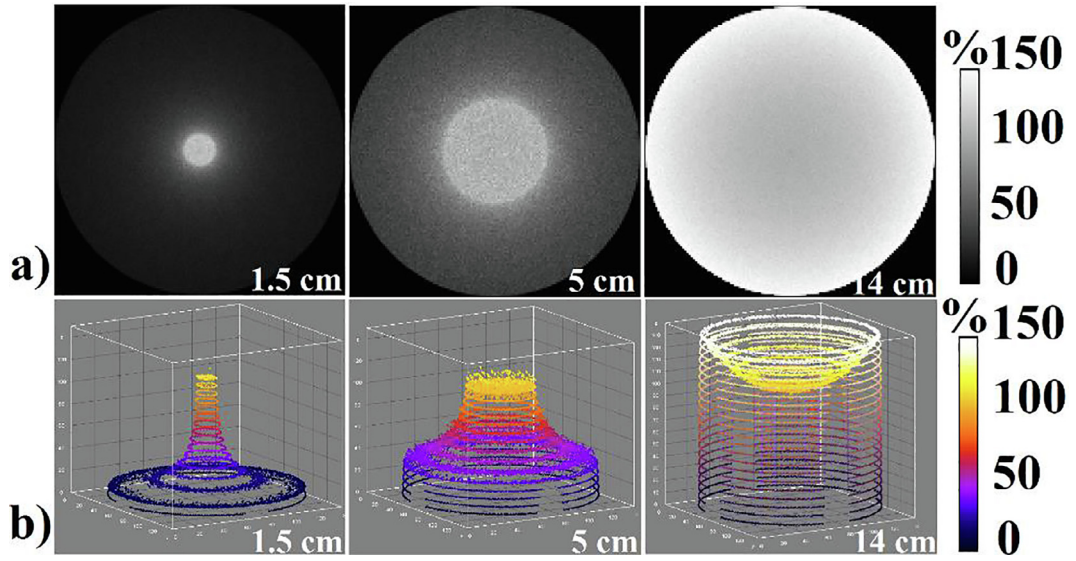

Fig. 9. a) 2D dose distribution (relative to dose at isocenter) in the central slice of a PE cylindrical phantom (14 cm diameter, 20 cm height) irradiated with different beam widths (1.5, 5, 14 cm, respectively from left side to right side) and 2 cm beam height at isocenter. b) 3D surface dose plot for 1.5, 5, 14 cm beam width (from left to right). Tube voltage: 320 kV, HVL = 4.4 mm Cu.

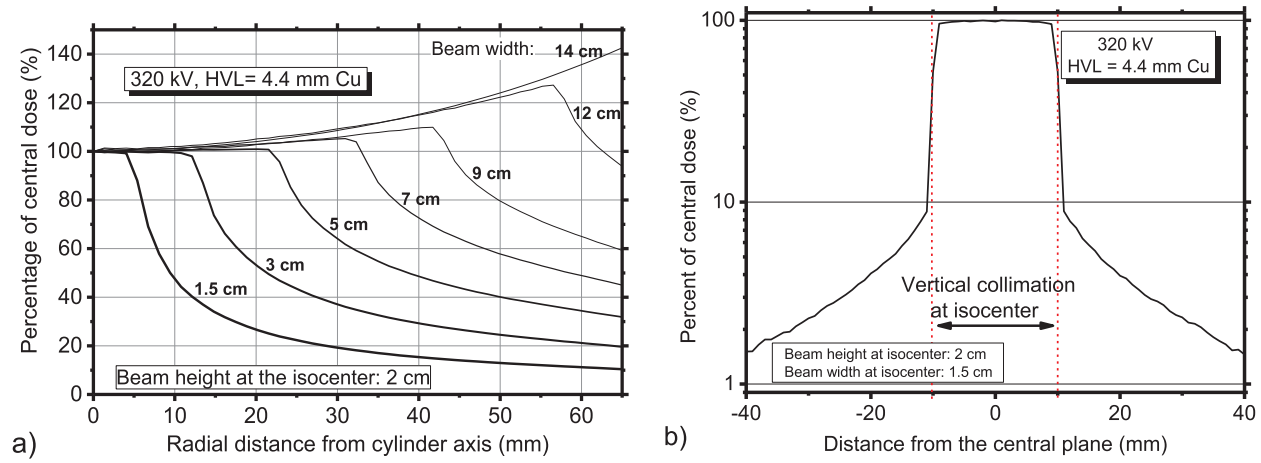

Fig. 10. a) Radial dose profiles, expressed as percentage of the central dose value, versus the radial distance in the phantom in a 14 cm diameter PE cylindrical phantom for different beam widths. b) Dose vertical profile for a collimation of 1.5 cm in the horizontal plane.

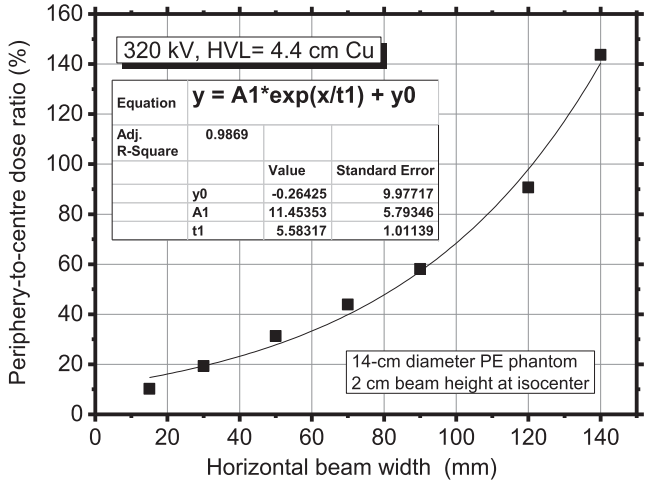

Fig. 11. Periphery-to-center dose ratio as a function of beam width. The continuous line describes an exponential growth of the percentage edge-to-center dose ratio with the increasing beam width at isocenter.

azimuthal direction in order to present a width of 1.0, 3.0, 7.0 or 14.0 cm at the scanner isocenter. Fig. 3 shows the adopted setup. Dose distributions were simulated with our MC code with a voxel size of $0.1 \times 0.1 \times 1.0\ cm^3$ and produced by integrating the dose along 10 cm.

2.5. Dose distribution at 320 kV

The dose distribution in the phantom was assessed via MC simulations using a 320 kV (HVL = 4.4 mm of copper) X-ray spectrum. Radial dose distributions obtained with different beam widths were evaluated in a homogenous PE phantom of 14 cm diameter and 20 cm height (this height simulates the overall breast length from chest wall to nipple and the presence of the patient body). The axis of rotation was coincident with the cylinder longitudinal axis and the X-ray beam was collimated in the transverse and longitudinal directions with respect to this axis. Simulation were achieved for 1.5, 3.0, 5.0, 7.0, 9.0, 12.0, 14.0 cm beam width in azimuthal direction and a beam height of 2.0 cm. Radial dose profiles were calculated in the irradiated slices, with a scoring resolution of $0.1 \times 0.1 \times 0.1\ cm^3$. Dose profiles (as percentage of central dose) were derived as a function of the radial distance from the cylinder axis; the periphery-to-center dose ratio was also estimated, for various

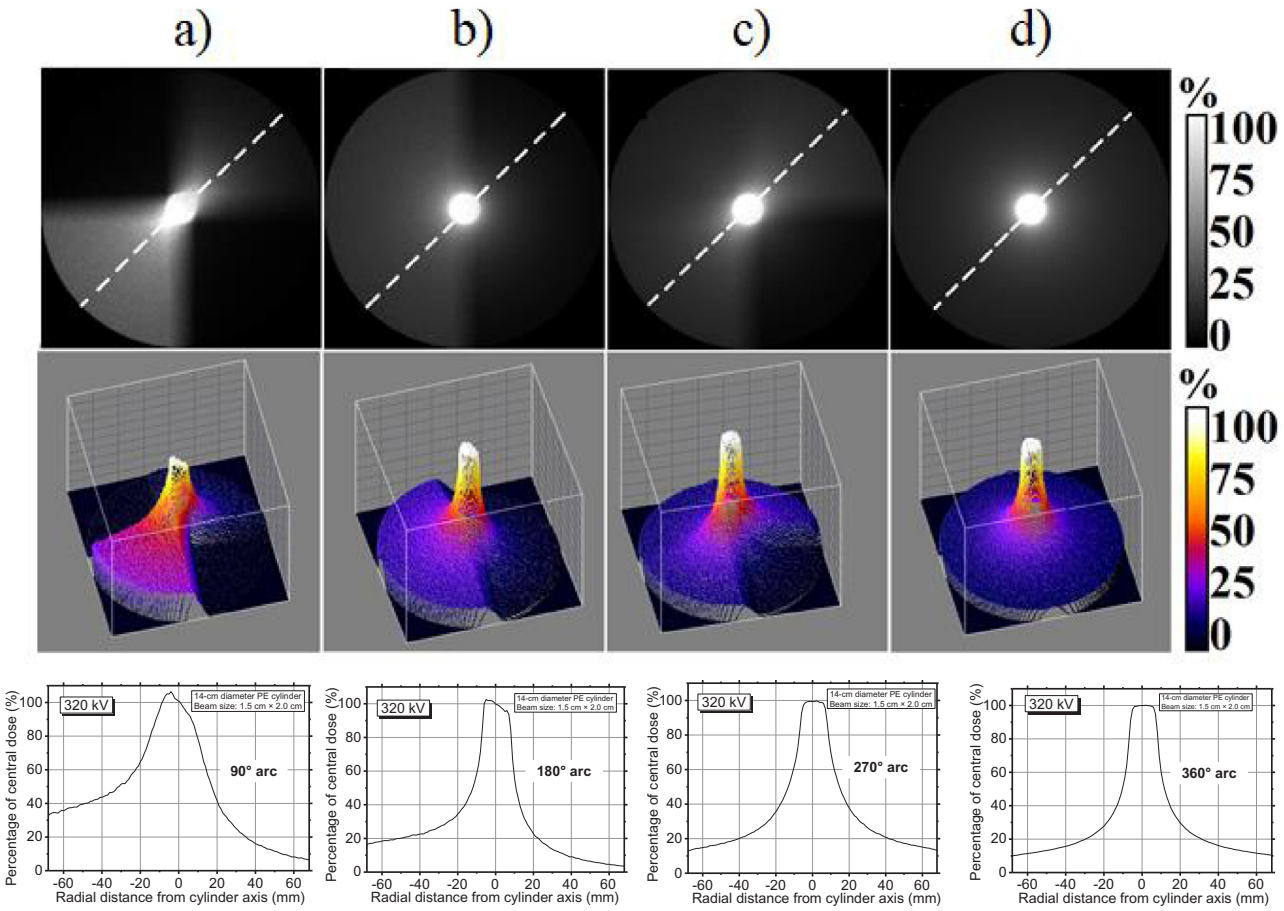

Fig. 12. 2D dose maps in coronal planes (top row), 3D surface dose plots (middle row) and dose line profiles (bottom row) (evaluated along the broken lines indicated in the gray-scale plots) for 320 kV (HVL = 4.4 mm Cu) X-ray beam, collimated to 1.5 cm × 2.0 cm (H × V), irradiating a PE phantom of 14-cm diameter and 15 cm height. a) Dose delivery on an arc of 90 deg with 1 deg increments; b) irradiation over 180 deg; c) irradiation over 270 deg; d) full irradiation over 360 deg. Number of photons launched = 10^5 per 1 deg angular step. Values are normalized to the dose at the isocenter.

beam widths.

2.5.1. Dose distribution at 320 kV (short scan)

We investigated also the delivery of the treatment on a scan arc shorter than 360 deg. For this purpose, we launched simulations with the point source rotating over 90, 180 or 270 deg (1 deg step) and evaluated the resulting 3D dose maps. For each simulation we launched 10^5 photons/deg.

2.5.2. Dose distribution at 320 kV (breast tissue)

The skin sparing effect expected from the rotational technique was evaluated in a heterogeneous phantom irradiated with a 320 kV X-ray spectrum, with a tumor modelled as a cylinder of 1.5 cm diameter and 2.0 cm height, and with a glandular fraction of 75%. We simulated the pendant breast as a 14.0 cm diameter cylindrical phantom of 0%, 50% or 100% glandular fraction by weight. For each type of breast composition three tumor positions were simulated, at various distances of the tumor axis from the central axis of the breast phantom. In particular, we considered a tumor with a tumor-to-cylinder axis distance of 0 cm (tumor at cylinder axis), 3.25 cm, or 5.25 cm. For irradiating the target volume, the beam size was 1.5 × 2.0 cm^2 (H × V), with the center of rotation along the tumor axis. The skin-to-tumor dose ratio was calculated to evaluate the skin sparing effect, and 3D dose distributions in the heterogeneous phantoms were derived from MC simulations, by evaluating the 20 1-mm thick irradiated slices.

2.5.3. Tube current modulation

When the tumor is located close to the surface of the breast the radial dose profile is not symmetrical, due to the shielding action of the breast tissue furthest from the lesion when the source is in the angular positions opposed to the lesion. This produces also an increase of the skin-to-tumor dose ratio. Moreover, the dose profile internal to the tumor becomes asymmetric, with the highest dose on the side closest to the breast wall. We investigated the possibility of modulating the current of the X-ray tube during the rotation of the source, simulating an increase of the tube current in angular positions at 180 deg with respect to the position of the tumor, located at 5.25 cm from the cylinder axis. The purpose was to improve dose homogeneity in the lesion, as well as to obtain additional skin dose sparing. We simulated the irradiation over 360 deg (with the 320 kV X-ray spectrum) of a heterogeneous cylinder (14 cm diameter, 20 cm height, 50% glandular fraction) containing a lesion of 1.5 cm diameter, 2.0 cm height and 75% glandular fraction. The cylindrical tumor volume was irradiated in a single rotation of the source with the vertical axis of rotation passing through the tumor center (Fig. 4b). The MC code was modified in such a way that for each angle of rotation (1 deg step) of the source, a 3D dose map was produced with 0.1 × 0.1 × 0.1 cm^3 resolution. We launched 10^6 photons/deg for 360 angular positions, uniformly distributed all around the breast; we simulated the modulation of the current in post-processing, by weighing the 3D dose distribution at each angular step with the weight function given by the “tube current modulation profile” shown in Fig. 4a (representing a sinusoidal modulation of the incident air kerma at the isocenter). The number of photons/deg was adjusted to

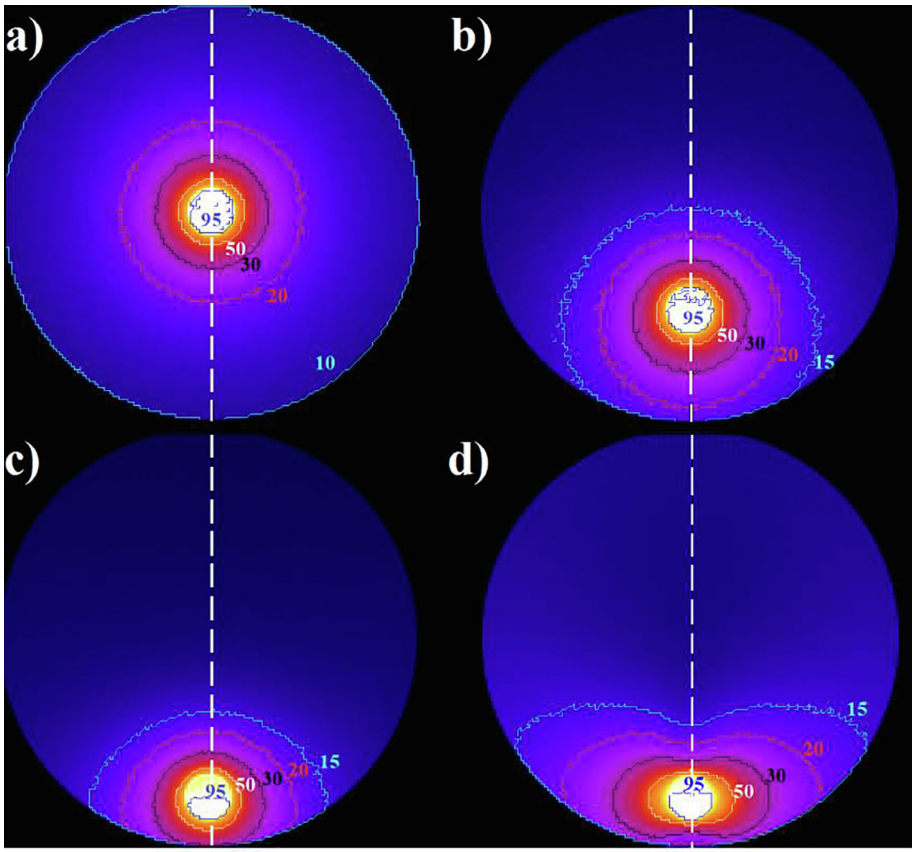

Fig. 13. Isodose curves in the coronal plane of the irradiated model breast containing the lesion at a) the cylinder axis, b) at 3.25 cm from the cylinder axis, c) at 5.25 cm from the cylinder axis and d) at 5.25 cm from the cylinder axis, with the current modulated following Fig. 4. The lesion was simulated as 75% glandular tissue and the breast was made of 50% glandular tissue. Tube voltage = 320 kV, HVL = 4.4 mm Cu.

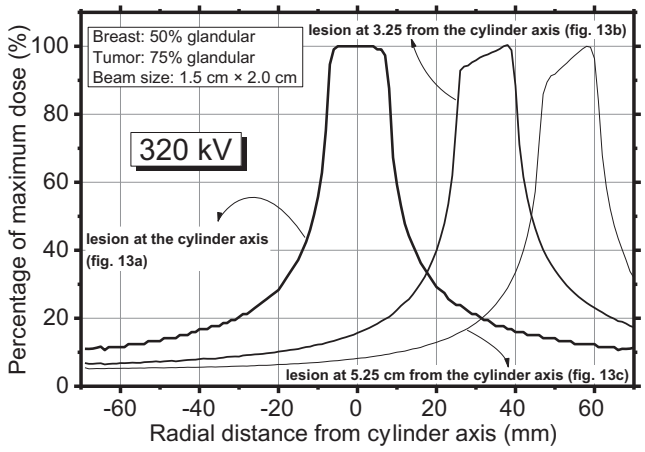

Fig. 14. Line dose profiles evaluated along the dashed line in Fig. 13a–c.

compensate for attenuation changes, due to different thicknesses of tissues traversed at each irradiation angle. A line dose profile was derived in the irradiated slices and compared with the one obtained without the tube current modulation.

3. Results

3.1. Validation of the MC code

Fig. 5 shows the simulated radial dose profiles for a monoenergetic X-ray beam at 178 keV computed with the code adopted in this work, compared to those in Ref. [1]. The percentage of central dose (dose normalized to the value at the center of rotation of the system) was plotted as a function of the radial distance from the isocenter. It was computed for a PE cylinder with a diameter of 14 cm. The mean difference was less than 3%. For a beam collimation of 1 cm at the isocenter, we estimated a periphery-to-center dose ratio of 7%.

Table 1
Average dose to target, maximum dose to skin and skin-to-tumor dose ratio for a lesion (1.5 diameter, 2.0 cm tall) placed at 0, 3.25 or 5.25 cm from the axis of the cylinder for different values of glandular weight fraction. The lesion was simulated as 75% glandular.

Tumor-to-cylinder axis distance (cm)	Breast glandular fraction by mass (%)	Average target dose (10^{-7} μGy/photon)	Maximum skin dose (10^{-7} μGy/photon)	Skin-to-tumor dose ratio (%)
0	50	1.12	0.12	10.7
0	100	1.10	0.12	10.9
0	0	1.20	0.13	10.8
3.25	50	1.27	0.20	15.7
3.25	100	1.22	0.22	18.0
3.25	0	1.31	0.22	16.8
5.25	50	1.50	0.51	34.0
5.25	100	1.47	0.51	34.7
5.25	0	1.53	0.53	34.6

3.2. Dose distributions at 150 kV

Fig. 6 shows radial dose profiles as a function of the distance from the isocenter for a collimated X-ray beam with a 150 kV spectrum. MC simulated data are plotted as lines and calculated as radial average profile on the cylinder coronal irradiated planes in order to reduce fluctuations; measured data are reported as dot points. A periphery-to-center dose ratio of 164%, 58%, 19%, 13% at 6.5 cm from the cylinder axis was estimated via MC simulations for beam width of 15, 7, 2.1, 1.4 cm, respectively. A mean percentage difference between data points and MC simulations was obtained as the average value of the

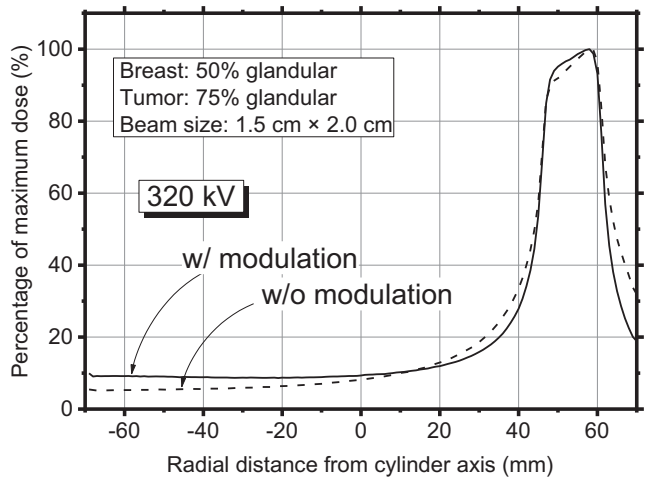

Fig. 15. Dose line profiles for tumor lesion at 5.25 cm from the axis of the cylinder, with and without tube current modulation. Line profiles were evaluated along the dashed line in Fig. 13c and d.

percentage differences at fixed beam collimation. Values of 21.6%, 12.6%, 2.2%, 0.9% for 1.4, 2.1, 7, 15 cm beam width were observed, respectively. A monoenergetic beam at 63 keV produced the same radial dose profile obtained for a 150 kV X-ray spectrum (Fig. 7).

3.3. Dose distribution at 300 kVp

Fig. 8 shows radial dose profiles estimated in this work via MC simulations with those measured in a previous work [11] with a 10 cm ionization chamber for various beam widths (1, 3, 7, or 14 cm) at fixed beam height of 10 cm and a spectrum of 300 kVp. MC simulations indicate a periphery-to-center dose ratio from 9% to 113% for horizontal beam collimations of 1 cm and 14 cm, respectively. The mean percentage difference between simulated dose profiles and experimental points was 1.8%, 2.7%, 9.7, and 20% for 1, 3, 7, 14 cm beam width, respectively.

3.4. Dose distribution at 320 kV

Fig. 9 shows 2D dose distributions and 3D surface dose plots for a collimated beam irradiating a 14-cm diameter PE phantom. They were evaluated in the central coronal planes. 2D dose maps are displayed in grey scale and normalized to the dose at the isocenter. As the beam width becomes narrower, the dose map results in a distribution focused at the center of rotation of the system. As shown in 3D surface dose maps, the percentage dose distribution changes from a peaked-shape (for a narrow-collimated beam, with high dose gradient between the center and the edge of the phantom), to a cupped-shape (for a broad beam) with the maximum dose deposit at the edge.

Fig. 10a shows average radial profiles plotted as percentage of central dose, for a beam width varying from 1.5 cm to 14.0 cm. The beam height in the axial direction was 2.0 cm. Radial dose distributions show an inversion of their shape from a cup-shaped profile (when the phantom was totally irradiated, with a dose value at the phantom edge of about 140% as much as that at the center of rotation), to a peaked distribution (when the phantom was irradiated with a narrow beam). With a 1.5 cm beam width, about 10% of the central dose was deposited at the edge of the phantom; the corresponding dose profile along the vertical direction (Fig. 10b) shows dose tails due to scatter in the phantom, up to 2 cm from the central irradiated slice of the cylindrical phantom. In order to estimate the skin sparing effect, the periphery-to-center dose ratio was plotted as a function of the beam width (Fig. 11). For 1.5 cm beam width, the ratio was about 1:10, for increasing horizontal collimation the ratio shows an exponential growth: it becomes about 4:10 for 7.0 cm beam width and 14:10 for 14.0 cm beam width.

3.4.1. Dose distributions at 320 kV (short angle scan)

Fig. 12 shows 2D dose distributions in the central coronal plane of a homogenous 14-cm diameter cylinder irradiated with 320 kV X-ray spectrum.

Fig. 12a shows the result of the dose delivery scheme when the source moves over an arc of 90 deg: note that, the dose distribution in the irradiated target volume does not present a circular shape. For the 180 deg and 270 deg dose delivery schemes (Fig. 12b, c) the dose distribution in the target has a round shape, but the dose distribution does not present a cylindrical symmetry as in the case of 360 deg scan (Fig. 12d). The larger the arc along which the source rotates around the target volume, the more uniform and symmetric becomes the dose distribution (Fig. 12, bottom row).

3.4.2. Dose distribution at 320 kV (breast tissue)

Fig. 13a,b,c show isodose curves in the coronal planes of the irradiated cylindrical breast models for a source spectrum of 320 kV tube voltage and an X-ray beam of 1.5 × 2.0 cm^2 (H × V) at the isocenter. The tumor lesion was made of 75% glandular breast tissue, with a background of 50% glandular breast tissue. The tumor lesion was placed at the axis of the cylinder (Fig. 13a), at 3.25 cm (Fig. 13b) or at 5.25 cm (Fig. 13c) from the axis of the cylinder. The isodose curves in the coronal plane through the center of the lesion indicate that in the first two configurations (Fig. 13a, b), the tumor receives a fraction of 95%, or higher, of the peak dose. The larger the distance from the axis of the cylinder and from the lesion, the larger the dose variance within the lesion, as shown in the dose profiles plotted in Fig. 14.

As shown, the maximum dose deposition (for the breast with a deep tumor at the cylinder axis) occurs at the center of rotation: the corresponding dose profile is flat along the 1.5-cm size of the lesion and the dose at the edge of the phantom is about 11% of the maximum dose. For off-center tumors, the farther the tumor axis to the cylinder axis, the lower the ratio between dose to the tumor and dose to the skin. For the tumor lesion at 5.25 cm from the axis of the cylinder, the relative skin dose ratio was 34% (Fig. 14).

Table 1 shows dosimetric data for the breast phantoms containing target lesions of 1.5 cm diameter and 2.0 cm height, positioned at different lesion-to-cylinder axis distances. Dose-to-target (average value over the entire lesion), maximum dose-to-skin and skin-to-tumor dose ratio were calculated for each type of breast composition and lesion. For the case of a deep target at the cylinder axis, the skin-to-tumor dose ratio ranges between 10.7% and 10.9%; the highest skin sparing was found in the case of 50% glandular breast. For the case of the superficial lesion (at 5.25 cm from the axis of the cylinder), the skin-to-tumor dose ratio was between 34.0% and 34.7%: it ranged between 15.7% and 18.0% for the target placed at 3.25 cm from the axis of the cylinder.

3.5. Tube current modulation

Fig. 15 shows the comparison between the simulated dose line profile obtained introducing the tube current modulation (in the treatment of a superficial lesion distant of 5.25 from cylinder axis) and that achieved in the same phantom without the modulation. The current modulation partially compensates for the lack of dose uniformity in the lesion at 5.25 cm from the axis of the cylinder (Fig. 13d). This effect can be noted also from Fig. 15, where the dose profile across the lesion becomes flatter with the current modulation. In addition, the current modulation permitted to reduce the dose to the skin, which passed from 34% of the maximum dose without current modulation, down to 20% with current modulation, as estimated from profiles in Fig. 15.

Fig. 16 shows dose histograms evaluated within the tumor in the same configuration of Fig. 13. The mean tumor dose, when compared to the maximum dose, reduces as the distance of the lesion from the cylinder axis increases. The mean tumor dose is 90.4% of the maximum

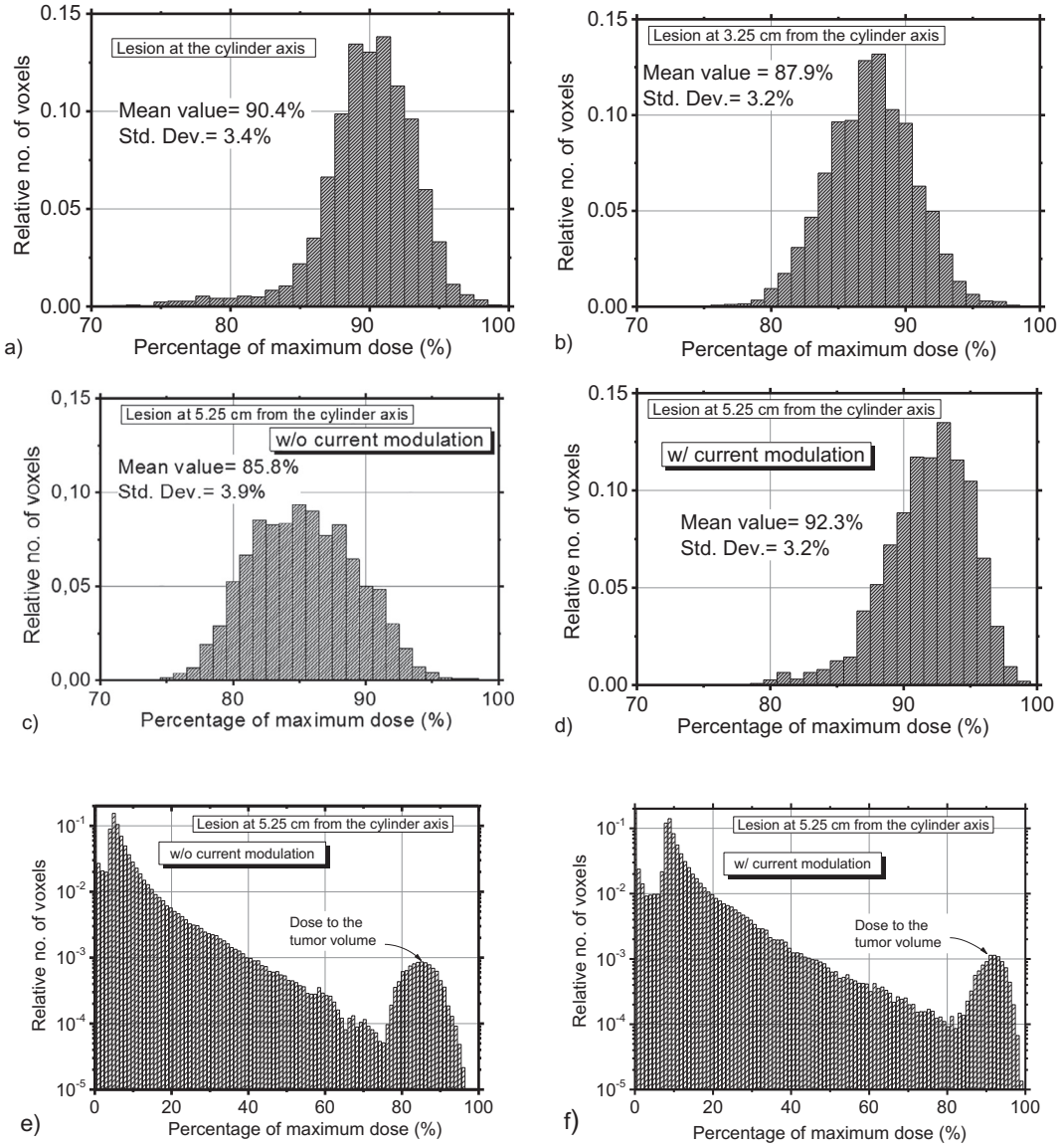

Fig. 16. Dose histogram within the tumor lesion a) at the cylinder axis, b) at 3.25 cm from the cylinder axis and at 5.25 cm from the cylinder axis c) without and d) with the tube current modulation. Dose histograms within the entire phantom volume with the tumor at 5.25 cm from the cylinder axis are shown in panel e) without, and in panel f) with, the tube current modulation.

dose value for the lesion located at the cylinder axis and it reduces to 87.9% and 85.8% for lesion at 3.25 cm and 5.25 cm from the axis of the cylinder, respectively. For the lesion at 5.25 cm from the cylinder axis, the modulation of the beam quantity reduces the dose spread around the mean dose to a value of 3.2% (evaluated as the standard deviation of the dose histogram), from a spread of 3.9% obtained without tube current modulation. The dose histograms evaluated on the whole slab (including normal tissue and the lesion) containing the simulated lesion are shown in Fig. 16e, f, showing the shift towards higher maximum dose and the shrinking of the dose distribution in the target region, with (Fig. 16f) and without (Fig. 16e) the tube current modulation, respectively.

4. Discussion

Following the initial suggestion by the UC Davis team [1], we investigated the use of a rotating platform which embodies a conventional X-ray tube and a suitable beam collimation system, as an alternative to using a linear accelerator, for RT of breast tumors. With the patient in prone position lying on a bed which can rotate around a vertical axis and translate horizontally, the X-ray source rotating around the breast lesion is collimated in order to irradiate the sole target volume placed at the scanner isocenter, via the rotational summation of the delivered dose at the lesion which permits dose sparing at the surface of the breast (skin tissue sparing).

Following the setup proposed in Ref. [1], we developed a Monte Carlo code and performed a series of measurements in order to evaluate the magnitude of the skin sparing factor and the dose distribution within the breast for different beam collimation, irradiation geometry (partial or total scan over 360 deg), tube voltage (320 kV, 300 kVp or 150 kV) and the possibility of modulating the photon fluence for reducing the skin dose for lesions close to the border surface. The shape of the dose distribution in a cylindrical phantom depends on the beam collimation in the direction perpendicular to the phantom axis. In particular, it is possible to obtain a dose accumulation around the axis of rotation, with a rapid fall off for a narrow beam: the periphery-to-center dose ratio was 7%, for a beam width of 1 cm at the isocenter and a monoenergetic photon beam at 178 keV. The difference of the simulated periphery-to-center dose ratio between our results and those in Ref. [1] for 178 keV is 3%, on average.

MC results showed a periphery-to-center dose ratio of about 9% for a 300 kVp beam collimated to 1.0 cm in the coronal plane; the value of 10% was obtained for a 320 kV beam collimated to 1.5 cm. Adopting a lower tube voltage of 150 kV (1.4 cm beam width) we showed that a 14-cm diameter cylinder could be irradiated with a periphery-to-center dose ratio as low as 13%, higher than the previous value at 320 kV but still acceptable for comparison with a conventional breast RT treatment with MV beams. The value of 13% is comparable with that (14%) obtained in Ref. [10] evaluated at 60 keV with monochromatic Synchrotron radiation under similar irradiation conditions. The radial dose profile computed for an X-ray tube operating at 150 kV was equivalent to that produced with a monoenergetic X-ray beam at 63 keV.

We observed that the closer the tumor lesion to the skin border, the higher the skin-to-tumor dose ratio; moreover, the target dose spread is larger for lesions close to the skin. We showed that these effects can be compensated for, via modulation of the X-ray tube output (e.g. tube current modulation). Indeed, MC simulations showed that for a breast modelled as a cylinder with a diameter of 14 cm and a lesion located at 5.25 cm from the cylinder axis, the skin-to-tumor dose ratio reduced from 34% (no tube current modulation) to 20% when the intensity of the rotating source is reduced while the source is at shortest radial distances from the lesion. At the same time, the dose spread within the lesion reduced from 3.9% to 3.2%, i.e. a more uniform target irradiation can be produced.

Conventional breast EBRT relies on a linac for producing high energy photon beams, this requiring a bunker for radioprotection reasons. This adds to the cost of the apparatus. Using an orthovoltage X-ray tube as the RT source would offer a less expensive solution to breast RT, by drastically reducing therapy costs both in terms of cost of the apparatus and maintenance and in terms of radioprotection issues [4]. Hence rotational kV-EBRT might also be of interest for treatments in middle and low-income Countries [17,18]. A further validation of the kV-EBRT irradiation technique (with a 100-keV monoenergetic beam) is ongoing within an experiment at the Australian Synchrotron, using 3D printed anatomically realistic breast phantoms derived from BCT patient scans acquired at UC Davis, manufactured in our lab with three components (PVA, ABS and Nylon) simulating, respectively, the absorption of skin, adipose and glandular tissue [19], also embedding a digitally printed tumor target volume: results will be reported in a future work.

5. Conclusion

We explored the possibility of breast kV-EBRT with X-ray tubes operating at high voltages down to 150 kV. Our simulations were in agreement with published results for a polyenergetic beam at 320 kV (and corresponding monoenergetic beam at 178 keV). We showed that adopting even lower energy spectra and collimated beams, we can reach consistent dose sparing at the skin, for small lesions. This would permit to lower the requirements on the orthovoltage X-ray tube, in terms of weight, cost, complexity of the beam collimation system, radioprotection issues. For 300 kVp spectrum collimated in order to irradiate an area with a diameter of 1 cm located at the center of the modelled breast, the calculated periphery-to-center dose ratio was 9%. A similar test for a 150 kV spectrum produced a dose ratio of 13%. For tumor lesions closer to the skin a higher skin-to-tumor dose ratio is produced; tube current modulation during the treatment showed to compensate for such an increase. Rotational kV-EBRT for the breast with the patient in prone position is still an experimental technique at the level of preliminary laboratory study, but its potential advantages motivate further research in this direction, also in view of a low-cost alternative to conventional accelerator-based breast RT.

References

[1] Prionas ND, McKenney SE, Stern RL, Boone JM. Kilovoltage rotational external beam radiotherapy on a breast computed tomography platform: a feasibility study. Int J Radiat Oncol Biol Phys 2012;84(2):533–9.

[2] Podgorsak EB. Radiation oncology physics: a handbook for teachers and students. Vienna: IAEA; 2005. p. 170–2.

[3] Sarno A, Mettivier G, Russo P. Dedicated breast computed tomography: basic aspects. Med Phys 2015;42(6):2786–804.

[4] Sarno A, Mettivier G, Di Lillo F, Cesarelli M, Bifulco P, Russo P. Cone-beam micro computed tomography dedicated to the breast. Med Eng Phys 2016;38(12):1449–57.

[5] National Surgical Adjuvant Breast and Bowel Project (NSABP), & Radiation Therapy Oncology Group (RTOG). A randomized phase III study of conventional whole breast irradiation (WBI) versus partial breast irradiation (PBI) for women with stage 0, I, or II Breast Cancer. Available online at: http://rpc.mdanderson.org/rpc/credentialing/files/B39_Protocol1.pdf.

[6] Bazalova – Carter M, Weil MD, Breitkreutz DY, Wilfley BP, Graves EE. Feasibility of external beam radiation therapy to deep-seated targets with kilovoltage X-rays. Med Phys 2017;44(2):597–607.

[7] Breitkreutz DY, Weil MD, Zavgorodini S, Bazalova-Carter M. Monte Carlo simulations of a kilovoltage external beam radiotherapy system on phantoms and breast patients. Med Phys 2017;44(12):6548–59.

[8] Breitkreutz DY, Renaud MA, Seuntjens J, Weil MD, Zavgorodni S, Bazalova – Carter M. Inverse optimization of low-cost kilovoltage X-ray arc therapy plans. Med Phys 2018;45(11):5161–71.

[9] Di Lillo F, Mettivier G, Sarno A, Castriconi R, Russo P. Towards breast cancer rotational radiotherapy with synchrotron radiation. Phys Med 2017;41:20–5.

[10] Di Lillo F, Mettivier G, Castriconi R, Sarno A, Stevenson AW, Hall CJ, et al. Synchrotron radiation external beam rotational radiotherapy of breast cancer: proof of principle. J Synchrotron Rad 2018;25:857–68.

[11] De Lucia PA, Kilovoltage Rotational External Beam Radiation Therapy (kV-EBRT) for breast cancer treatment. (M.Sc. Thesis (Physics)), University of Naples Federico II, 2015. Available online at: http://www.infn.it/thesis/thesis_dettaglio.php?tid=10622.

[12] Sarno A, Masi M, Antonelli N, Di Lillo F, Mettivier G, Castriconi R, et al. Dose volume distribution in digital breast tomosynthesis: a phantom study. IEEE Trans Rad Pl Med Sci 2017;1:322–8.

[13] Sarno A, Mettivier G, Di Lillo F, Bliznakova K, Sechopoulos I, Russo P. Homogeneous vs. patient specific breast models for Monte Carlo evaluation of mean glandular dose in mammography. Phys Med 2018;51:56–63.

[14] Sarno A, Mettivier G, Tucciariello RM, Bliznakova K, Boone JM, Sechopoulos I, et al. Monte Carlo evaluation of glandular dose in cone-beam X-ray computed tomography dedicated to the breast: homogeneous and heterogeneous breast models. Phys Med 2018;51:99–107.

[15] Sarno A, Mettivier G, Russo P. Air kerma calculation in Monte Carlo simulations for deriving normalized glandular dose coefficients in mammography. Phys Med Biol 2017;62:N337–49.

[16] Sechopoulos I, Ali ES, Badal A, Badano A, Boone JM, Kyprianou IS, et al. Monte Carlo reference data sets for imaging research: executive summary of the report of AAPM research committee task group 195. Med Phys 2015;42:5679–91.

[17] Datta NR, Samiei M, Bodis S. Radiation therapy infrastructure and human resources in low- and middle-income countries: present status and projections for 2020. Int J Radiat Oncol Biol Phys 2014;89:448–57.

[18] Abdel-Wahab M, Fidarova E, Polo A. Global access to radiotherapy in low- and middle-income countries. Clin Oncol 2016;29:99–104.

[19] Ivanov D, Bliznakova K, Buliev I, Popov P, Mettivier G, Russo P, et al. Suitability of low density materials for 3D printing of physical breast phantoms. Phys Med Biol 2018;63(17):175020.